


ARTICLE



WNT2–SOX4 positive feedback loop promotes chemoresistance and tumorigenesis by inducing stem-cell like properties in gastric cancer

Xiang-Yu Tan^{1,5}, Yu-Ting Li^{1,2,5}, Hua-Hui Li^{1,2}, Li-Xiang Ma¹, Chui-Mian Zeng³, Tian-Tian Zhang¹, Tu-Xiong Huang¹, Xiao-Di Zhao⁴ and Li Fu¹ 

© The Author(s), under exclusive licence to Springer Nature Limited 2023

Gastric cancer (GC) is characterized by its vigorous chemoresistance to current therapies, which is attributed to the highly heterogeneous and immature phenotype of cancer stem cells (CSCs) during tumor initiation and progression. The secretory WNT2 ligand regulates multiple cancer pathways and has been demonstrated to be a potential therapeutic target for gastrointestinal tumors; however, its role involved in gastric CSCs (GCSCs) remains unclear. Here, we found that overexpression of WNT2 enhanced stemness properties to promote chemoresistance and tumorigenicity in GCSCs. Mechanistically, WNT2 was positively regulated by its transcription factor SOX4, and in turn, SOX4 was upregulated by the canonical WNT2/FZD8/ β -catenin signaling pathway to form an auto-regulatory positive feedback loop, resulting in the maintenance of GCSCs self-renewal and tumorigenicity. Furthermore, simultaneous overexpression of both WNT2 and SOX4 was correlated with poor survival and reduced responsiveness to chemotherapy in clinical GC specimens. Blocking WNT2 using a specific monoclonal antibody significantly disrupted the WNT2–SOX4 positive feedback loop in GCSCs and enhanced the chemotherapeutic efficacy when synergized with the chemo-drugs 5-fluorouracil and oxaliplatin in a GCSC-derived mouse xenograft model. Overall, this study identified a novel WNT2–SOX4 positive feedback loop as a mechanism for GCSCs-induced chemo-drugs resistance and suggested that the WNT2–SOX4 axis may be a potential therapeutic target for gastric cancer treatment.

Oncogene (2023) 42:3062–3074; <https://doi.org/10.1038/s41388-023-02816-1>

INTRODUCTION

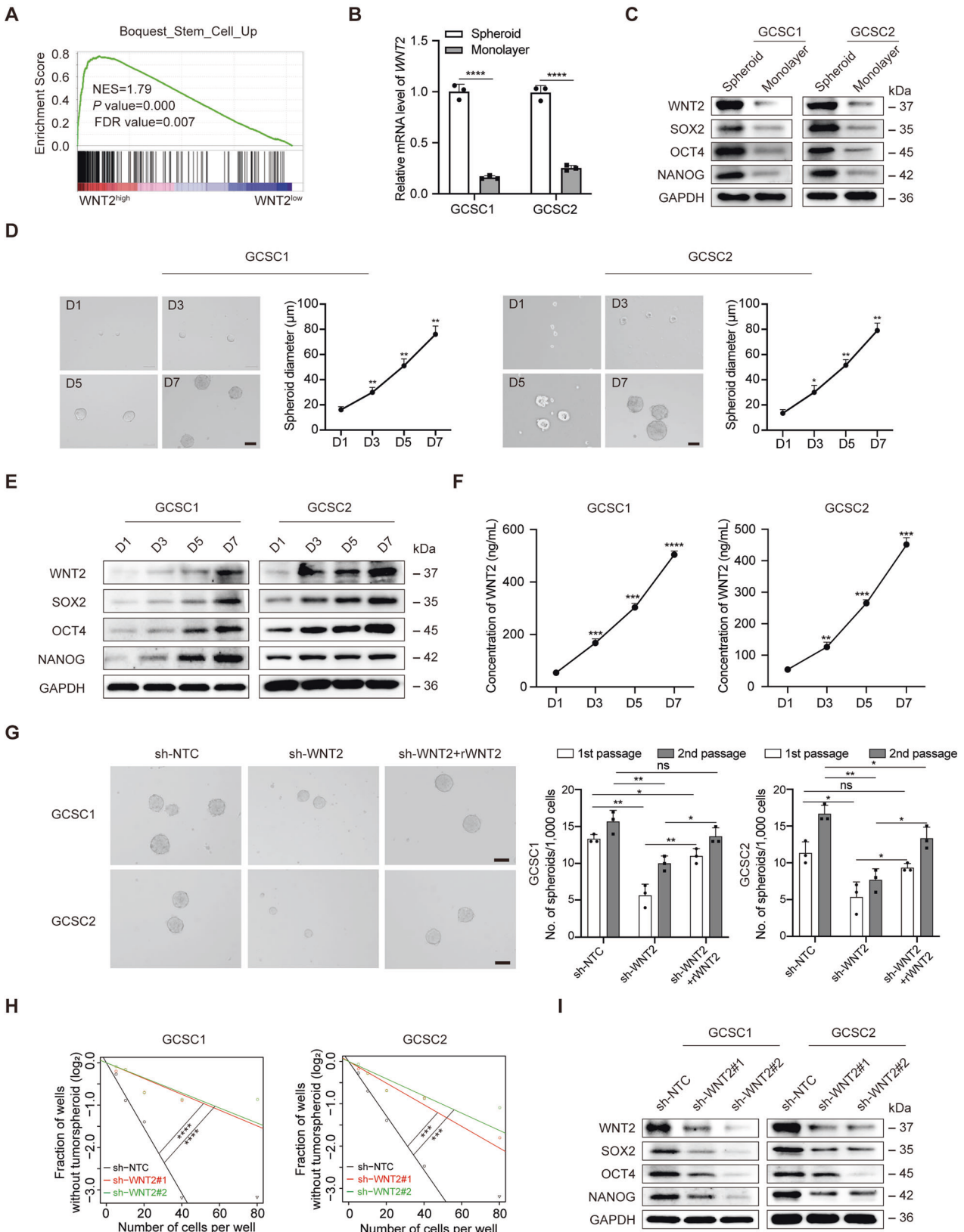
Gastric cancer (GC) is one of the most frequently diagnosed malignancies worldwide and has high mortality [1]. Chemotherapy improves patients' survival and quality of life with locally advanced unresectable or metastatic gastric cancer [2]. However, most cases with relapsed or distant metastases have multidrug resistance after treatment [3], suggesting that targeting the bulk of tumor cells might not be sufficient. There is substantial evidence that intratumor heterogeneity affects traditional chemotherapeutic responses, highlighting the urgent need to develop novel treatments for advanced gastric cancer. In recent decades, a variety of cancer stem cell (CSC) populations have been comprehensively characterized within the complex tumor micro-environment (TME) of GC [4] and were found to be responsible for maintaining solid tumor heterogeneity [5]. Moreover, gastric carcinogenesis is a multistep process initiated by CSCs [6], which maintains its self-renewal ability by developing treatment-resistant clones during the progression of relapse [7]. As such, an efficacious and specific gastric CSCs (GCSCs)-targeted therapy is needed to completely eliminate gastric cancer.

Recent strategies targeting GCSCs have shown promise in reducing their populations [8], inhibiting tumor growth, and increasing tumor responses to chemotherapy [9]; however, studies evaluating the safety and efficacy and underlying mechanism of the therapy *in vivo* are still underway [10]. Most importantly, the biological molecular mechanisms underlying the effects of GCSCs on primary human tumor tissues and recurrence after chemotherapy remain incompletely illustrated. The WNT/ β -catenin pathway, a highly conserved embryonic developmental-signaling pathway, is commonly altered in gastric cancer, and its continuous activation directs symmetric cell division in the self-renewal of several cancer CSCs [11, 12]. Indeed, the aberrant activation of WNT-signaling target genes [13, 14] and an enhanced gastric CSCs-like phenotype have also been observed in gastrointestinal CSCs [15]. The vital member of the WNT family, WNT2, is an evolutionarily conserved glycoprotein ligand secreted by cells, and a profusion of evidence has demonstrated that the overexpression of WNT2 is closely linked with stepwise carcinogenesis progression in multiple malignant gastrointestinal cancers [16, 17]. Recent studies showed that

¹Guangdong Province Key Laboratory of Regional Immunity and Diseases, Department of Pharmacology and International Cancer Center, Shenzhen University Medical School, Shenzhen University, Shenzhen 518055 Guangdong, China. ²Shenzhen University-Friedrich Schiller Universität Jena Joint PhD Program in Biomedical Sciences, Shenzhen University Medical School, Shenzhen University, Shenzhen 518055 Guangdong, China. ³Department of Endocrinology and Diabetes Center, The First Affiliated Hospital of Sun Yat-sen University, Guangzhou 510080 Guangdong, China. ⁴Xijing Hospital of Digestive Diseases, Fourth Military Medical University, Xi'an 710032 Shaanxi, China. ⁵These authors contributed equally: Xiang-Yu Tan, Yu-Ting Li. ✉email: gracelfu@szu.edu.cn

Received: 16 November 2022 Revised: 14 August 2023 Accepted: 18 August 2023

Published online: 26 August 2023



overexpression of circOSBPL10 or circLMO7 could contribute to the high transcriptional level of WNT2 in GC cells, and overexpression of WNT2 had a significant positive correlation with worse GC prognosis [18, 19] and lymph node metastasis [20].

However, there is little evidence indicating whether WNT2 production has a role in GCSC self-renewal and cancer chemotherapy or which regulatory mechanisms achieve stemness maintenance and the tumorigenic potential of GCSCs.

Fig. 1 **WNT2 promotes the stem cell-like properties in GCSCs.** **A** GSEA enrichment plot of expression of genes associated with stem cells in high WNT2 versus low WNT2 expressing GC samples in the TCGA dataset ($n = 415$). **B** Transcriptional levels of *WNT2* in GCSCs of spheroid and monolayer status ($n = 3$). **C** Protein expression levels of WNT2, SOX2, OCT4, and NANOG in GCSCs of spheroid and monolayer status, as detected by western blot. **D** GCSC spheroids were photographed and morphology and diameters (μm) were measured on day (D) 1, 3, 5, and 7; scale bar, 50 μm ($n = 3$). **E** Expression levels of WNT2 and key stemness-associated proteins examined by western blot in GCSCs on day (D) 1, 3, 5 and 7. GAPDH was used as an internal control. **F** ELISA measurement of GCSC supernatant WNT2 levels on D 1, 3, 5, and 7 ($n = 3$). **G** Representative photomicrographs of sh-WNT2-transfected GCSCs, or sh-WNT2-transfected GCSCs rescued by rWNT2 (50 ng/mL); scale bar 50 μm (left). Tumor spheroid formation assay indicated that silencing of WNT2 decreased the spheroid formation of GCSCs but was partially increased by additional rWNT2 treatment for 1 week. Secondary spheroids formed from dissociating spheroids also demonstrated a similar trend, but with enhanced serial spheroid-forming capacity as indicated (right) ($n = 3$). **H** In vitro limiting dilution assays showing effects of WNT2 on the spheroid formation of GCSCs ($n = 3$). **I** Immunoblots for WNT2 and stemness-associated proteins in WNT2-silenced GCSCs. The error bars are presented as the means \pm SD. n.s. not significant; * $P < 0.05$; ** $P < 0.001$; *** $P < 0.001$; **** $P < 0.0001$. NTC non-target control.

Although WNT2 is expressed in human fetal organs during development, it is almost undetectable in normal adult tissues, except during tumorigenesis [21]. This indicates that WNT2 is a promising therapeutic target, and WNT2-targeted therapies have important clinical implications in cancer chemo-drug treatment [22, 23]. However, it is unknown whether anti-WNT2 therapy can suppress GCSCs and overcome GCSC-mediated chemoresistance. In the present study, we set out to elucidate the role of secreted WNT2 in regulating GCSC properties and the underlying mechanisms by which WNT2 promotes gastric cancer stemness and tumorigenesis, and to explore a new way to regulate WNT2 levels to improve chemotherapeutic efficacy for gastric cancer patients.

RESULTS

Overexpression of WNT2 contributes to the stemness maintenance of GCSCs

To study the role of WNT2 in regulating stemness properties in GC, we initially examined the protein level of WNT2 in four GC cell lines (AGS, HGC-27, MKN-45, and MGC-803) and one immortalized normal gastric epithelial cell line GES-1. As compared to the GES-1, WNT2 was remarkably upregulated in all the 4 GC cell lines examined (Supplementary Fig. 1A). GES-1 and MGC-803 cells cultured as spheroids present a significantly increased WNT2 accompanied by elevated expression of three well-known stemness-related markers (SOX2, OCT4, and NANOG) compared to those cells cultured as a monolayer. (Supplementary Fig. 1B, C). Notably, WNT2 expression in GC patients-derived GCSC1 and GCSC2 cells that were validated by both CD44 and CD54 expression (Supplementary Fig. 1D), was found to be prominently upregulated in their spheroid status compared with the monolayer status (Supplementary Fig. 1E), indicating that high WNT2 expression may be involved in the stemness regulation of GCSCs.

Furthermore, an enrichment plot showed that high expression of WNT2 is significantly associated with cancer stemness (Fig. 1A). Next, we observed a striking increase of WNT2 mRNA level in GCSCs grown as spheroids compared with those grown in monolayer (Fig. 1B). In addition, the stemness-related markers were increased along with the elevation of WNT2 protein in GCSCs grown as spheroids (Fig. 1C). Interestingly, the time-dependent increase in the diameter of the GCSC spheroids was well correlated with increasing WNT2 protein expression; meanwhile, the expression of stemness-related markers was also increased gradually with WNT2 elevation in GCSCs in a time-dependent manner (Fig. 1D, E). As WNT2 is a secretory protein, we verified that the secretion of WNT2 into the culture media of GCSCs was also increased in this time-dependent self-renewal process (Fig. 1F). To further confirm whether WNT2 is a functional marker of GCSCs, we knocked down the endogenous WNT2 expression in GCSCs (GCSC1/2-sh-WNT2) by lentiviral transduction. Non-template short hairpin RNA-transfected (GCSC1/2-sh-NTC) cells were used as controls, respectively. A significant decrease in spheroid-forming capabilities was found in WNT2-repressed GCSC

cells (Fig. 1G, H), which was partially rescued by the treatment of recombinant human WNT2 protein (rWNT2) (Fig. 1G). In addition, the expression of stemness-related markers (SOX2, OCT4 and NANOG) was also remarkably decreased in WNT2-repressed GCSC cells compared with control cells (Fig. 1I).

WNT2 promotes the chemoresistance, epithelial-mesenchymal transition (EMT) and tumor growth in GCSCs

Cancer stem cells are postulated mediators of chemoresistance, we thus look into the influence of WNT2 on the chemoresistance in GCSCs. As shown in Fig. 2A, the knockdown of WNT2 significantly reduced the IC50 value to 5-FU, OXA, and cisplatin (DDP) in GCSCs, which was partially rescued by the treatment of rWNT2. Moreover, the knockdown of WNT2 in GCSCs conferred chemosensitivity to genotoxic treatments (5-FU + OXA or 5-FU + DDP), which was also partially rescued by the treatment of rWNT2 (Fig. 2B). Meanwhile, the knockdown of WNT2 in GCSCs remarkably inhibited the process of EMT (Fig. 2C). Moreover, to investigate the tumorigenic potential of WNT2-repressed GCSCs in vivo, sh-NTC- or sh-WNT2-GCSCs were subcutaneously engrafted into nude mice. The results showed that the knockdown of WNT2 significantly delayed the GCSC-derived tumor growth (Fig. 2D–F). Collectively, these findings point to a clear scenario in which, on the one hand, WNT2 overexpression in GCSCs conferred chemoresistance to genotoxic therapies, while on the other hand, WNT2 engendered the GCSC more aggressive tumorigenicity in vivo.

SOX4 transactivates WNT2 to promote GCSC stemness and chemoresistance

To further explore the molecular mechanisms underlying the upregulation of WNT2 transcript level in GCSCs, we evaluated the gene expression levels of top 9 significantly upregulated transcription factors (TFs) in CD44+ CD54+ WNT2+ compared with CD44+ CD54+ WNT2- cells by analyzing the GC single-cell (sc) RNA-seq dataset (GSE183904) (Fig. 3A). Among the top 9 TFs, only 4 genes, including *SOX4*, *HIF1A*, *EEA1*, and *RARA*, were significantly overexpressed in GC tissues compared with normal gastric tissues (Supplementary Fig. 2). Notably, CD44+ CD54+ WNT2+ cells exhibited a significantly high expression level of SOX4, an essential developmental TF that has been shown to be frequently amplified and is known to regulate stemness in various types of malignancies [24]. We then checked whether SOX4 and WNT2 proteins are simultaneously expressed in CD44+ CD54+ GCSCs by double IF staining. The results showed that both WNT2 and SOX4 were highly expressed and colocalized in GCSC cells (Fig. 3B). In an effort to identify potential WNT ligands regulated by SOX4, we assessed the transcriptional levels of 18 human WNT ligands in SOX4-knockdown GCSC cells. Among the 18 ligands, the expression of 6 downstream WNT genes was profoundly affected by silencing SOX4 (Supplementary Fig. 3A). Interestingly, after assessing correlations of these 6 WNT genes with SOX4 and subsequent differential expression of the 6 WNT genes in GC, we found SOX4 showed a positive correlation solely with WNT2 in the

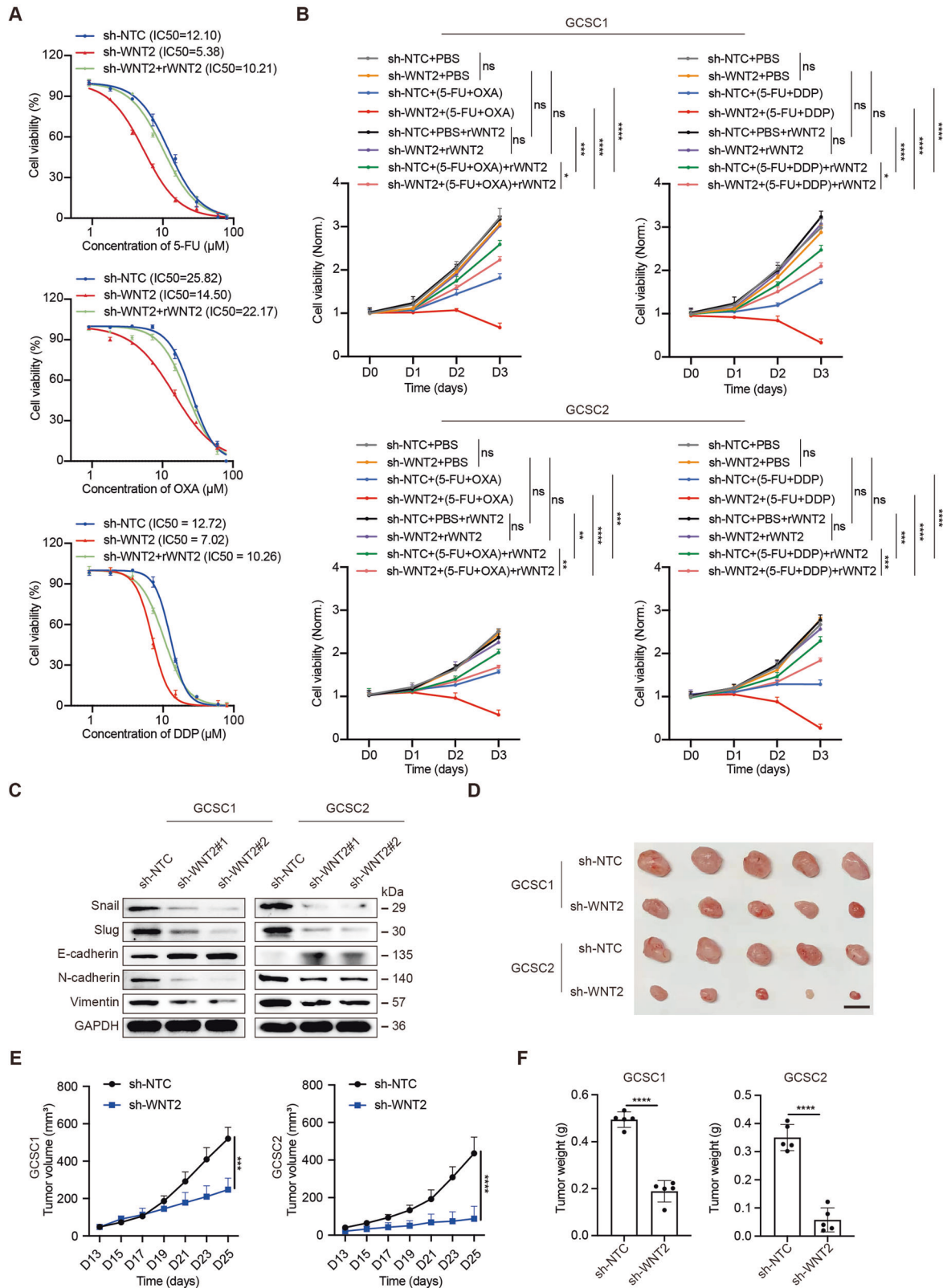
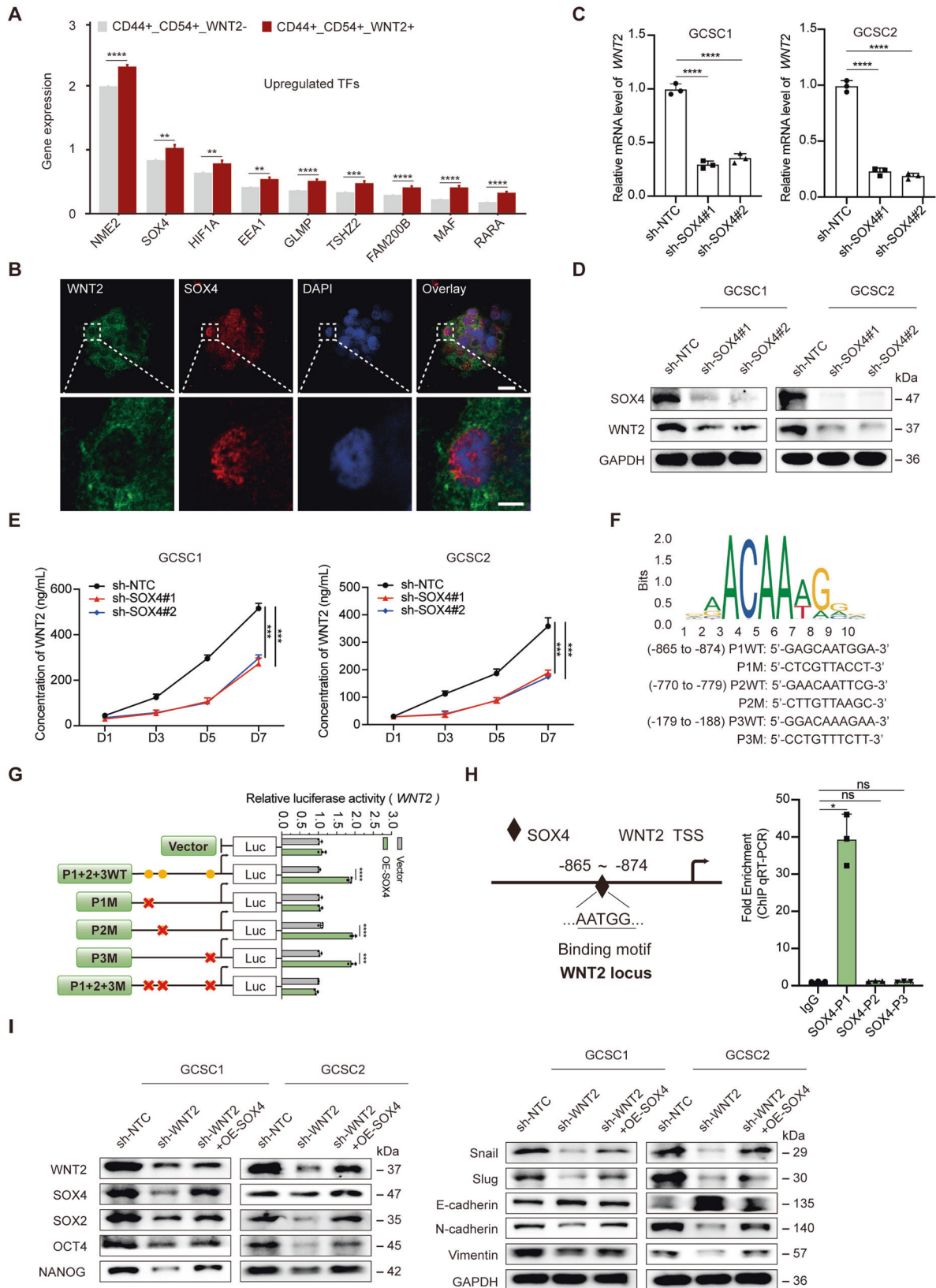


Fig. 2 Knockdown of WNT2 inhibits chemoresistance, EMT, and tumor growth in GCSCs. **A** CCK8 assay determination of IC50 of 5-FU, OXA, and DDP in WNT2-silenced GCSCs rescued by rWNT2 (50 ng/mL) ($n = 3$). **B** Cell viability analyses of WNT2-silenced GCSCs rescued by rWNT2 (50 ng/mL) after 5-FU plus OXA and 5-FU plus DDP treatment ($n = 3$). **C** Immunoblots of EMT-related proteins in WNT2-silenced or control GCSCs. **D–F** Subcutaneous xenograft tumor formation in vivo in nude mice from GCSC1/GCSC2 transfected sh-NTC or sh-WNT2 (sh-WNT2#2) ($n = 5$). Tumors were harvested after 25 days, and representative images are shown (**D**); scale bar, 1 cm. Charts show changes in tumor volumes, monitored every 2 days, in two groups of mice (**E**). Changes in tumor weight were detected at the end of the experiment in the two groups of mice (**F**). Knockdown of WNT2 drastically suppressed tumor growth in vivo. The error bars are presented as the means \pm SD. n.s. not significant; * $P < 0.05$; ** $P < 0.01$; *** $P < 0.001$; **** $P < 0.0001$.



TCGA STAD database (Supplementary Fig. 3B, C), indicating that SOX4 may transactivate WNT2 in GCSCs. As expected, silencing SOX4 dramatically decreased WNT2 mRNA (Fig. 3C), protein (Fig. 3D), and secretory levels (Fig. 3E) in GCSCs.

Using the online tool JASPAR and the UCSC genome browser, it turned out that SOX4 was predicted to have three binding sites with the promoter region of WNT2, including -865--874 bp (P1: GAGCAATGGA), -770--779 bp (P2: GAACAATTCG) and

Fig. 3 WNT2 was transcriptionally regulated by SOX4 in GCSCs. **A** GC scRNA-seq dataset (GSE183904) analysis demonstrated the gene expression levels of the top 9 upregulated TFs in CD44+ CD54+ WNT2+ cells versus CD44+ CD54+ WNT2- cells. **B** Immunofluorescence analysis of WNT2 and SOX4 in GCSC cells; scale bar, 20 μ m (top); scale bar, 5 μ m (bottom). **C** qPCR ($n = 3$), Western blot (**D**) and ELISA (**E**) ($n = 3$) analysis of WNT2 at mRNA, intracellular and secretory protein levels in sh-SOX4#1/#2-transfected GCSCs and control GCSC cells. **F** Predicted SOX4 binding sites of the WNT2 promoter obtained using UCSC genome browser (<http://genome.ucsc.edu/>) and JASPAR database (<http://jaspardev.genereg.net>). **G** Luciferase reporter assay detection of the binding region of SOX4 in the WNT2 promoter in 293T cells ($n = 3$). **H** Schematic showing predicted SOX4 binding sites of the WNT2 promoter region (left). The ChIP-qPCR assay showed that SOX4 is directly bound to a specific site in the WNT2 promoter in GCSC1 cells (right) ($n = 3$). **I** Western blot analysis of WNT2, SOX4, stemness- and EMT-associated markers for SOX4 protein overexpression rescue experiments in WNT2-silenced GCSCs. The error bars are presented as the means \pm SD. n.s. not significant; * $P < 0.05$; ** $P < 0.01$; *** $P < 0.001$; **** $P < 0.0001$. P1WT wild type of position 1; P1M mutation of position 1; P2WT wild type of position 2; P2M mutation of position 2; P3WT wild type of position 3; P3M mutation of position 3; P1 + 2 + 3WT, wild type of position 1 + 2 + 3; P1 + 2 + 3M, mutation of position 1 + 2 + 3.

–179–188 bp (P3: GGACAAAGAA) (Fig. 3F). We then performed luciferase reporter assays by constructing five WNT2 promoter reporters that included all three predicted SOX4-binding sites with WNT2 promoter and their individually or simultaneously mutated binding sites. The results showed that SOX4 transactivates WNT2 by binding its promoter at the P1 region (Fig. 3G). The ChIP-qPCR assay also demonstrated that endogenous SOX4 protein directly binds to the promoter of WNT2 and specifically transactivates WNT2 in GCSC cells (Fig. 3H). Moreover, we overexpressed SOX4 in WNT2-repressed GCSCs and, consistent with the above observation, WNT2 was also rescued by SOX4 at the protein level in GCSCs (Fig. 3I). These findings suggested that overexpression of WNT2 is attributed to the transcriptional regulation of SOX4 in GCSCs.

Furthermore, we tested whether SOX4 plays a critical role in the WNT2-mediated stemness properties of GCSCs. As shown in Supplementary Fig. 4A, B, SOX4 was also overexpressed in GCSCs and MGC-803 grown as spheroid. Knockdown of SOX4 demonstrated strong stemness-repressing and EMT inhibition abilities in GCSCs (Supplementary Fig. 4C–F). Rescue experiments showed that the knockdown of SOX4-inhibited spheroid formation capability and EMT process was partially rescued by recombinant human WNT2 protein (rWNT2) (Fig. 4A–C). Moreover, the 5-FU, OXA, and DDP resistance ability of SOX4-repressed GCSC cells were significantly lower than control cells (Fig. 4D). Meanwhile, knockdown of SOX4 in GCSCs also conferred chemosensitivity to genotoxic treatments (5-FU + OXA or 5-FU + DDP) (Fig. 4E), suggesting that SOX4 takes an active role in WNT2-mediated stemness and chemoresistance of GCSCs.

WNT2–SOX4 feedback loop maintains stemness by activating canonical WNT/ β -catenin signaling in GCSCs

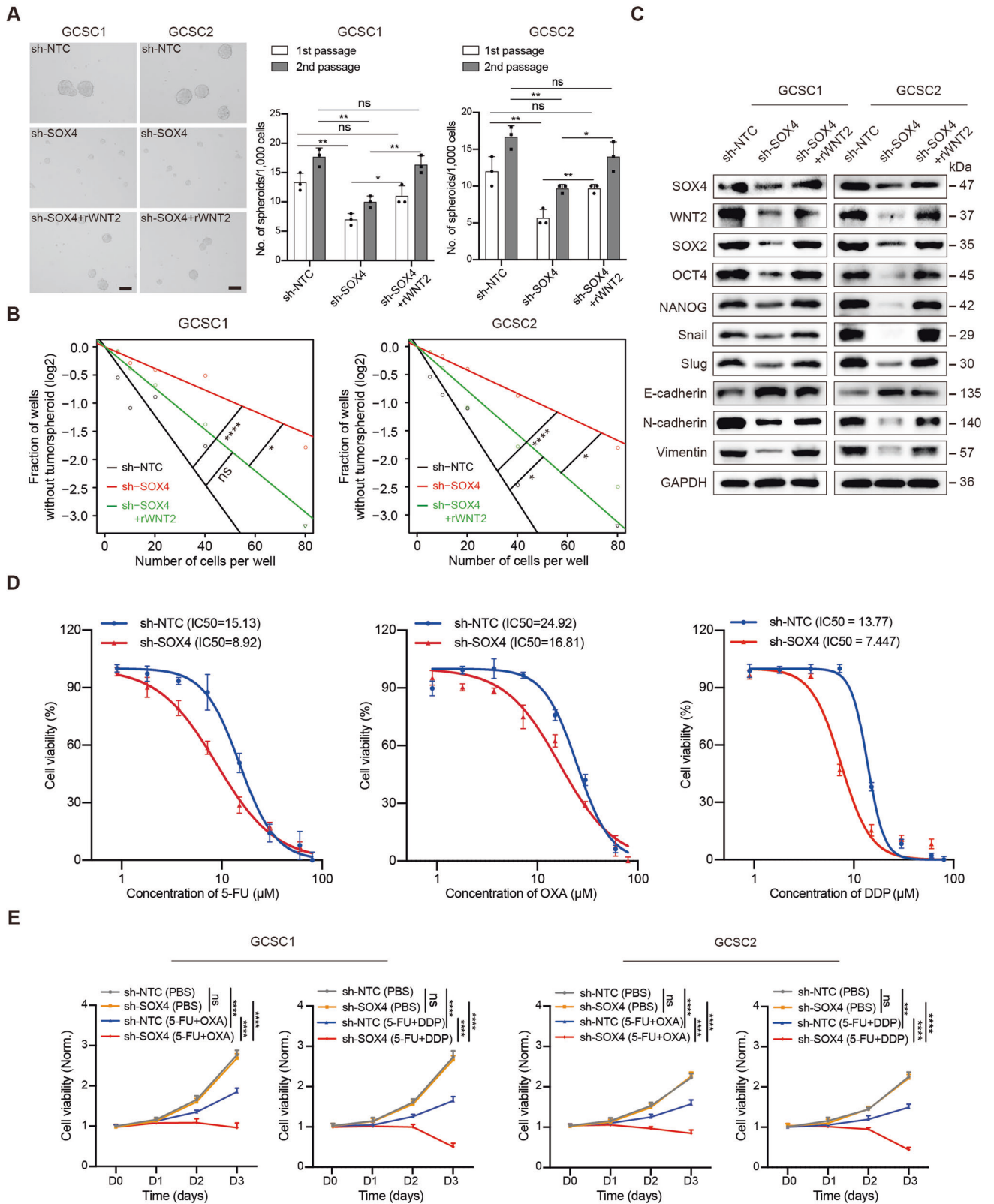
Aberrant activation of the WNT pathway co-occurs with the high expression of WNT ligands and receptors. To determine which FZD receptors specifically bind to the WNT2 ligand in GCSCs, we initially compared the mRNA expression levels of 10 human FZDs between the spheroid and differentiated monolayer GCSCs by qPCR. The results showed that FZD4, FZD5, and FZD8 were significantly upregulated in GCSCs grown as spheroids (Supplementary Fig. 5A). Next, by analyzing the correlations of these 3 FZDs with WNT2 or SOX4 in the TCGA STAD dataset, it turned out that only FZD8 was positively associated with both WNT2 and SOX4 in GC (Supplementary Fig. 5B, C). Interestingly, the FZD8 protein level was also remarkably upregulated in GCSC spheroids as compared to their monolayer status (Supplementary Fig. 5D). To further substantiate the role of FZD8 as the signal receptor and downstream effector of WNT2 in regulating GCSCs, we found that the WNT2 protein robustly interacted with the FZD8 protein (Supplementary Fig. 5E), and they were positively and significantly correlated in GC cells (Supplementary Fig. 5F). We further explored why FZD8 protein levels were protected by WNT2. The results showed that the FZD8 levels plummeted within 6 h of cycloheximide (CHX) treatment to block de novo protein synthesis in GCSCs; while FZD8 levels remain unchanged at different time points (0, 2, 3, 4, 5, 6 h) after CHX and rWNT2 co-treatment (Supplementary Fig. 5G). Additionally, a

concurrent significant increase in FZD8 protein levels was also highlighted by rWNT2 and proteasome inhibitor MG132 co-treatment compared to rWNT2 or MG132 treatment (Supplementary Fig. 5H). Furthermore, co-IP demonstrated that ubiquitination of the FZD8 protein was prominently reduced in response to rWNT2 treatment of GCSCs (Supplementary Fig. 5I), suggesting that WNT2 stabilizes FZD8 protein by attenuating its ubiquitination.

As expected, when we knocked down WNT2, both FZD8 and active β -catenin protein levels were significantly reduced in GCSCs (Fig. 5A). Notably, the knockdown of FZD8 in GCSCs decreased the expression levels of active β -catenin and SOX4 (Fig. 5B). More interestingly, both WNT2 and SOX4 protein levels were significantly decreased upon silencing of β -catenin, and these reductions were partially rescued by treatment of GCSCs with rWNT2 in GCSCs (Fig. 5C). Moreover, both FZD8 and β -catenin protein expression was also decreased upon silencing of SOX4, and these reductions were partially rescued by treatment of GCSCs with rWNT2 as well (Fig. 5D). Remarkably, decreased WNT2, SOX4, FZD8, and active β -catenin protein levels in GCSCs was partially rescued by the overexpression of SOX4 (Fig. 5E), suggesting that WNT2–FZD8– β -catenin–SOX4 forms a positive feedback loop in regulating GCSCs. Furthermore, we treated GCSCs with a specific anti-WNT2 monoclonal antibody (mAb) as reported in our previous study [25]. Similar to the effect conferred by WNT2-knockdown with shRNA, anti-WNT2 mAb demonstrated significantly decreased stemness properties of the GCSCs and diminished the activity of the WNT2–SOX4 feedback loop (Fig. 5F).

Previous studies have suggested that SOX4 plays a critical role in WNT signaling [24, 26]. Consistent with this notion, SOX4 has a highly positive correlation with signature gene sets relating to WNT/ β -catenin signaling in GC (Supplementary Fig. 6A). In addition, high FZD8 expression also showed a statistically significant association with EMT and stemness GSEA signatures (Supplementary Fig. 6B). This is consistent with the observation that FZD8 protein expression increased along with the natural accumulation of active β -catenin during GCSCs' self-renewal process in spheroids (Supplementary Fig. 6C). Notably, the stemness-promoting function in either FZD8- or β -catenin-repressed GCSCs are reduced concomitantly (Supplementary Fig. 6D–H); while both FZD8 and active β -catenin exhibited a strikingly consistent increase in GES-1 and MGC-803 spheroids (Supplementary Fig. 6I). These findings further confirmed that FZD8– β -catenin canonical signal fuels WNT2–SOX4 feedback loop in GCSC stemness regulation.

Additionally, we also explored whether WNT2 has an effect on GCSC stemness via the non-canonical WNT2/STAT3 signaling pathway as reported by our previous study in esophageal cancer cells [24]. The results showed that there was no change in protein levels of total STAT3 and p-STAT3 (Tyr705) between WNT2 knockdown and control GCSCs (Supplementary Fig. 7A). Meanwhile, the protein level of SOX4 was also not changed after the treatment with STAT3 inhibitor Napabucasin in GCSCs (Supplementary Fig. 7B). These results indicated that the activation of WNT2–SOX4 feedback loop was independent of the non-canonical WNT2/STAT3 signaling pathway in GCSCs.



Positive correlation between WNT2 and SOX4 expression in GC cohorts

To gain comprehensive insights into the correlation between WNT2 and SOX4 expression in human GC patients, we initially examined the expression of WNT2 in GC tumor tissues and normal

gastric tissues using Gene Expression Profiling Interactive Analysis (GEPIA). In line with the previous report [19], an overall upregulation of WNT2 was observed in GC (Supplementary Fig. 8A). Gene set enrichment analysis (GSEA) also showed that high expression of WNT2 was significantly and positively

Fig. 4 SOX4 contributes to WNT2-mediated stemness and chemoresistance in GCSCs. **A** Representative photomicrographs of sh-SOX4-transfected GCSCs, or sh-SOX4-transfected GCSCs rescued by rWNT2 (50 ng/mL). sh-NTC-transfected GCSCs was used as control; scale bar 50 μ m (left). Tumor spheroid formation assay indicated that silencing of SOX4 decreased the spheroid formation of GCSCs but was partially increased by additional rWNT2 treatment for 1 week. Secondary spheroids formed from dissociating spheroids also demonstrated a similar trend, but with enhanced serial spheroid-forming capacity as indicated (right) ($n = 3$). **B** In vitro limiting dilution assay showing rescue effects of rWNT2 in SOX4-silenced GCSCs ($n = 3$). **C** Western blot of SOX4, WNT2, stemness- and EMT-related markers in SOX4-silenced GCSCs with or without rWNT2 rescue for 72 h. **D** CCK8 assay of IC50 of 5-FU, OXA, and DDP in SOX4-silenced GCSCs ($n = 3$). **E** Cell viability analyses of SOX4-silenced GCSCs after 5-FU plus OXA and 5-FU plus DDP treatment ($n = 3$). The error bars are presented as the means \pm SD. n.s. not significant; * $P < 0.05$; ** $P < 0.001$; *** $P < 0.001$; **** $P < 0.0001$.

correlated with advanced GC (Supplementary Fig. 8B). Furthermore, we determined the clinical relevance of WNT2 and SOX4 protein levels by GC-TMA, respectively. IHC staining showed that both WNT2 (Supplementary Fig. 8C, D) and SOX4 (Supplementary Fig. 9A, B) protein levels were strikingly high in GC tumor tissues. Kaplan–Meier survival analysis revealed that high WNT2 (Supplementary Fig. 8E) or SOX4 (Supplementary Fig. 9C) expression was significantly correlated with poor overall survival of GC patients. Receiver operating characteristic (ROC) curve analysis for GC data from the corresponding datasets revealed both WNT2 (Supplementary Fig. 8F) and SOX4 (Supplementary Fig. 9D) expression levels may serve as a highly sensitive and specific diagnostic biomarkers for GC patients.

Consistent with the in vitro findings in GCSCs, WNT2 expression was significantly and positively correlated with SOX4 expression in GC patients (Fig. 5G, H). Kaplan–Meier survival analysis further revealed an increased probability of poor overall survival time for patients with both high WNT2 and high SOX4 expression (Fig. 5I). In addition, both high WNT2 and high SOX4 expression were significantly associated with advanced T stage and poor differentiation in GC (Supplementary Fig. 10A, B), suggesting that clinical GC patients with high-WNT2/SOX4 expressing tumors have a more dismal prognosis than those patients with low-expression of WNT2 or SOX4.

To gain insight into the relevance of WNT2 and SOX4 in GC chemoresistance, we collected 11 cases of paired biopsied or surgically resected tumor specimens from GC patients before and after neoadjuvant chemotherapy (Supplementary Table S3). The representative micrographs of H&E staining that led to the initial diagnosis of the 11 primary GC tumors were shown in the Supplementary Fig. 11. Among the 8 patients who did not respond to chemotherapy, double IF staining of WNT2 and SOX4 in post-chemotherapy tumors exhibited simultaneous increased expression compared with their pre-chemotherapy tumors (Fig. 5J). However, no significantly increased expression of WNT2 and SOX4 was observed in tumors from patients who responded to chemotherapy (Supplementary Fig. 12). Despite the small sample size, these findings indicated that the simultaneous overexpression of WNT2 and SOX4 is clinically linked to the acquired chemoresistance of GC.

Disrupting WNT2–SOX4 positive feedback loop enhances the therapeutic efficacy of 5-FU plus OXA in GC

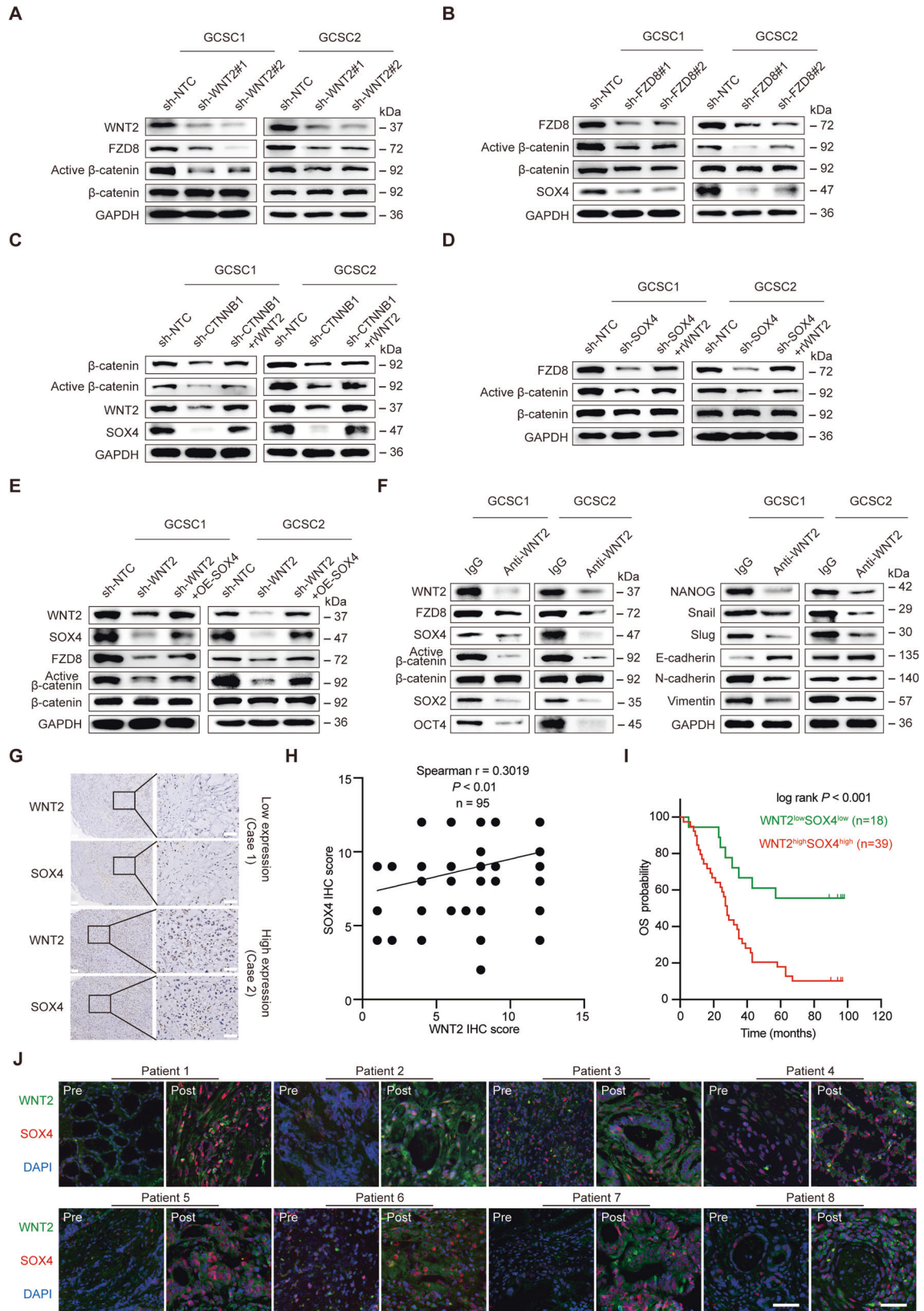
As both WNT2 and SOX4 showed strong resistance to 5-FU + OXA in GCSCs, we then explored whether disrupting the WNT2–SOX4 axis by using a specific anti-WNT2 mAb could sensitize a GCSC-initiated subset of tumors to 5-FU + OXA in vivo. Mice with established tumors were randomly assigned to receive treatment with either saline or IgG control, or anti-WNT2 mAb or 5-FU + OXA or a combination of both for 14 days (Fig. 6A). Mice harboring GCSC-derived xenografts treated with anti-WNT2 mAb or 5-FU + OXA showed significantly delayed tumor growth compared with the control group. Notably, combined treatment with both anti-WNT2 mAb and 5-FU + OXA was more efficacious and potent compared with 5-FU + OXA or anti-WNT2 mAb treatment in halting tumor growth and tumor weight (Fig. 6B–D); while no

obvious toxicity-related side effects were observed among the four treatment groups (Supplementary Fig. 13A, B).

Furthermore, H&E staining analysis revealed larger areas of cell death in GCSC xenografts treated with anti-WNT2 mAb alone or in combination with 5-FU + OXA than those in the control group (Fig. 6E). IHC staining also revealed that xenografts treated with anti-WNT2 mAb resulted in a marked reduction or increasing of key factors (WNT2, FZD8, active β -catenin, SOX4, E-cadherin, N-cadherin, and Vimentin) in the WNT2–SOX4-mediated feedback loop as compared to the control and 5-FU + OXA alone treatment group (Fig. 6E). Of note, the activation of WNT2–SOX4-mediated loop markers was significantly abrogated in tumors treated with anti-WNT2 mAb combined with 5-FU + OXA, which is consistent with the proliferation marker Ki67 expression among the four treatment groups (Fig. 6E). Collectively, these data demonstrated that 5-FU + OXA sensitization was a result of a decrease in the function of the WNT2–SOX4 signaling loop induced by anti-WNT2 mAb, which provides evidence that utilizing WNT2-neutralizing antibodies is a potential way to enhance the efficiency and efficacy of 5-FU + OXA.

DISCUSSION

CSCs are dynamic in status, and their functions in GC are complicated. Hence, targeting CSC pathways that induce EMT and/or account for the acquisition of tumor stemness may be more effective than strategies that only target the already existing CSCs [27]. Yet, the effect of WNT2 on the reciprocal crosstalk between GCSCs and the tumor microenvironment, as well as the mechanisms underlying the WNT2-mediated GCSC properties are still not fully comprehended. We and others have previously reported that WNT2 was upregulated in cancer-associated fibroblasts (CAFs) of esophageal cancer [25] and colorectal cancer [28], it's still unclear whether WNT2 was upregulated in CAFs of GC. A recent study illustrated the transcriptional profile of CAFs in GC [29]. CAFs-derived WNT2 was not significantly upregulated in poor outcomes versus favorable outcomes from the stroma of GC patients. In addition, WNT2 was also not upregulated in PDPN+ CAFs compared with control normal fibroblasts from triple-transgenic gastric cancer mice [29]. However, due to the heterogeneity of CAFs, it would be of interest to further investigate whether other types of CAFs overexpress WNT2 in GC. To the best of our knowledge, here we provide the first evidence that WNT2 accumulation is time-dependently in GCSCs and correlates with stemness maintenance and poor survival in GC patients. In line with our results, GES-1 cells infected with CagA-positive *Helicobacter pylori* and/or MNNG display CSC-like properties accompanied by a significantly upregulated WNT2 [30]. WNT2 can initiate intracellular signaling and participate in stem cell homeostatic maintenance and specification [24] in developmental processes. Previous studies have shown that WNT2 serves as a downstream molecule of miR-335-3p in triple-negative breast cancer [26] and miR-30a-3p [19] and circOSBPL10 [18] in GC. Yet, no functional transcriptional regulators of WNT2 have been reported. In this study, we disclosed that the transcription factor SOX4 can directly bind to the WNT2 promoter and activate its



transcription and elucidated the origin of aberrant WNT2 over-expression in GCSCs. The SOX4 gene has proved to be important for WNT signaling [31]. SOX4 is an essential developmental TF that regulates CSCs stemness [32, 33]. Previous studies also showed

that SOX4 is involved in regulating TGF- β -induced EMT and the stem cell characteristics of GC cells [34]. However, the regulatory relationship between WNT2 and SOX4 in GCSCs is not fully understood. Interestingly, we observed high levels of SOX4 in

Fig. 5 WNT2 maintains GCSC stemness by activating the WNT2-FZD8-SOX4 positive feedback loop. **A** Western blot analysis of WNT2, FZD8, active β -catenin, and β -catenin protein levels in WNT2-silenced GCSCs. **B** Immunoblotting of FZD8, active β -catenin, β -catenin and SOX4 proteins in lysates prepared from GCSCs transfected with FZD8 shRNAs (sh-FZD8#1 or sh-FZD8#2) or control shRNA (sh-NTC). **C** Western blot of rWNT2 rescue experiments in CTNNB1-silenced GCSCs. **D** Western blot of rWNT2 rescue experiments in SOX4-silenced GCSCs. **E** Immunoblotting of WNT2, SOX4, FZD8, active β -catenin, and β -catenin proteins in WNT2-silenced GCSCs with or without overexpression of SOX4. **F** Western blot showing protein expression of WNT2, FZD8, SOX4, active β -catenin, β -catenin, stemness- and EMT-related markers in GCSCs subjected to anti-WNT2 mAb treatment (200 μ g/mL) after 72 h. **G** Representative IHC staining of low and high expression of WNT2 and SOX4 in GC-TMA samples; scale bar, 100 μ m (left); scale bar, 50 μ m (right). **H** Spearman correlation analysis of WNT2 and SOX4 IHC score ($n = 95$, $P = 0.0029$). **I** Kaplan–Meier Plotter curve shows both high WNT2 and high SOX4 expression were associated with poorer survival of GC patients ($P < 0.001$). OS, overall survival. **J** Double-IF staining of WNT2 and SOX4 in 8 non-responsive human GC specimens obtained before and after chemotherapy. Scale bar, 50 μ m. The error bars are presented as the means \pm SD.

GCSCs when there was an accumulation of WNT2 and CSC markers. The continuous WNT2 protein production during the GCSC self-renewal procedure suggests that there is a regenerative feedback pattern that acts via interplays between WNT2 expression and intracellular signaling.

Aberrant WNT pathway activation caused by the overexpression of canonical FZD receptors and WNT ligands is present in a variety of cancers [35, 36]. Here, we showed that extracellular WNT2 binds to and stabilizes FZD8 via deubiquitylation, thereby activating β -catenin-mediated stemness. This is in line with the previous report that FZD8 is the putative WNT2 receptor of CAFs in colorectal cancer [28]. In the cytomembrane, FZD8 promotes bone metastasis in prostate CSCs [37]. Importantly, genome-wide promoter analysis showed that FZD8 is a high-confidence direct target gene of SOX4 in prostate cancer cells [32]. However, little is known about the upstream regulatory mechanism of SOX4 while WNT2 accumulates continually in GCSCs. Here, we provide the first data showing that activated WNT2/FZD8/ β -catenin signals significantly induce SOX4 expression. Moreover, previous studies have also strongly suggested that β -catenin interacts directly with SOX4 in a cooperative way to activate the downstream target genes [32, 33]. Collectively, this evidence represents the initial discovery of bidirectional regulation involving SOX4, FZD8, and β -catenin. This positive feedback loop is an efficient means by which GCSCs continually produce WNT2.

In the clinical aspect, we found that simultaneous overexpression of both WNT2 and SOX4 was correlated with poor survival and chemotherapy resistance of GC patients. Therefore, targeting the WNT2 production engine of WNT2–SOX4 may be a viable option for overcoming chemoresistance in GC. Fluoropyrimidine plus platinum-based chemotherapy is a widely preferred standard first-line treatment for the initial treatment of patients with advanced human gastric and gastroesophageal junction adenocarcinoma [38–40]. Novel agents targeting cancer stemness should complement the antitumor activity of chemotherapy by eliminating drug-resistant CSC or inhibiting the capacity of tumor cells to acquire features of CSCs [15, 41]. However, the critical role of WNT signaling in stem cell maintenance has raised concerns regarding the dose-limiting toxicity of WNT-targeting agents in bone, hair, and the gastrointestinal tract as well as in hematopoiesis, which has limited the clinical application of other pan-inhibitors [42, 43]. Of note, no WNT/FZD antagonists or WNT-ligand-specific mAbs targeting gastric cancer, especially on CSCs have been included in clinical trials [44]. Interestingly, based on our findings, the growth of GCSC-derived tumors was stalled in its progression by blocking the WNT2 generation cycle using a specific anti-WNT2 mAb developed in our group, with devastating stemness loss to the tumor, which dramatically revert tumor resistance to 5-FU and OXA. Similar to our previous findings, this WNT2-specific mAb has been demonstrated to act as a precise WNT2-targeting therapy and a safe way to exert a significant antitumor effect [25]. Therefore, anti-WNT2 mAb plus chemotherapy could be developed into an alternative treatment for GC patients. In doing so, anti-WNT2 mAb would have significant clinical implications by inhibiting seed CSCs and tumor recurrence

and lowering the dose of chemotherapy required for a small number of rapidly growing tumors. However, it is still unknown whether normal adult stem cells express WNT2, and the identification of a more specifically favorable therapeutic index dose of anti-WNT2 mAb that is not as equally toxic to normal gut stem cells will be required. In addition, as WNT2 is a secreted protein, a further investigation of whether the serum WNT2 concentration and differential SOX4 expression levels [45] are adaptable as a combined highly sensitive and specific therapeutic and prognostic supervision index for GC is warranted.

In conclusion, this study presented compelling evidence that GCSCs-auto-secreted WNT2 is crucial for sustaining the stemness properties of GCSCs, ultimately promoting chemoresistance and the tumorigenic process through a WNT2–SOX4 positive feedback loop, which may be effectively blocked by our specific anti-WNT2 mAb (Fig. 6F). Consequently, we have uncovered a novel WNT2–SOX4 positive feedback loop targeting therapeutic strategy that renders GCSCs eradicable with chemotherapy, leading to the inhibition of GC development and progression.

MATERIALS AND METHODS

Cell lines and human tissue samples

GC patient-derived CD44+ CD54+ GCSCs (GCSC1 and GCSC2) were kindly provided by Prof. Xianming Mo (Sichuan University). These cells were maintained in vitro as previously described [46]. The human 293T cell line was obtained from the American Type Culture Collection. The immortalized human normal gastric epithelial cell line GES-1 and human GC cell lines (AGS, HGC-27, MKN-45 and MGC-803) were obtained from Cobio Biosciences. 293T and GES-1 cell lines were maintained in DMEM (Gibco, NY, USA), and all GC cell lines were cultured in RPMI-1640 (Gibco). All media were supplemented with 10% fetal bovine serum (FBS; Gibco) and antibiotics (100 U/mL penicillin and 100 μ g/mL streptomycin; Gibco), and cells were incubated in humidified cell chambers (5% CO₂, 37 °C). All cell lines were recently authenticated by STR and mycoplasma- and chlamydia-negative.

All human GC samples were obtained from the Xijing Hospital of Digestive Diseases. The pathological information for the samples was provided by the Department of Pathology (Supplementary Table 3). We collected 11 pairs of tumor specimens before and after neoadjuvant chemotherapy. Pre-chemotherapy-treated specimens were obtained by biopsy under gastroscopy of patients with GC, and post-chemotherapy specimens were collected at the time of surgery. All human subjects provided informed consent, and Institutional Review Board approval was obtained for this study from Shenzhen University and Xijing Hospital.

Tissue microarray (TMA), Immunohistochemical (IHC), and Hematoxylin/Eosin (HE) analysis

The human GC-TMA (HStmA180Su17) of 95 patients (including 85 pairs of GC tissue samples matched to their adjacent samples) was purchased from Shanghai Outdo Biotech. All human subjects provided informed consent, and Institutional Review Board approval was obtained for this study from Shenzhen University and Shanghai Outdo Biotech. The TMA was incubated with anti-WNT2 antibody [25] (Kexing Biotech, custom-made, Hangzhou, China) or anti-SOX4 antibody (Abcam, ab86809, Cambridge, UK), and both were detected with the EnVision+ detection system (Dako, Copenhagen, Denmark) according to the manufacturer's instructions. WNT2- and SOX4-immunostained microarray assessment was independently performed by

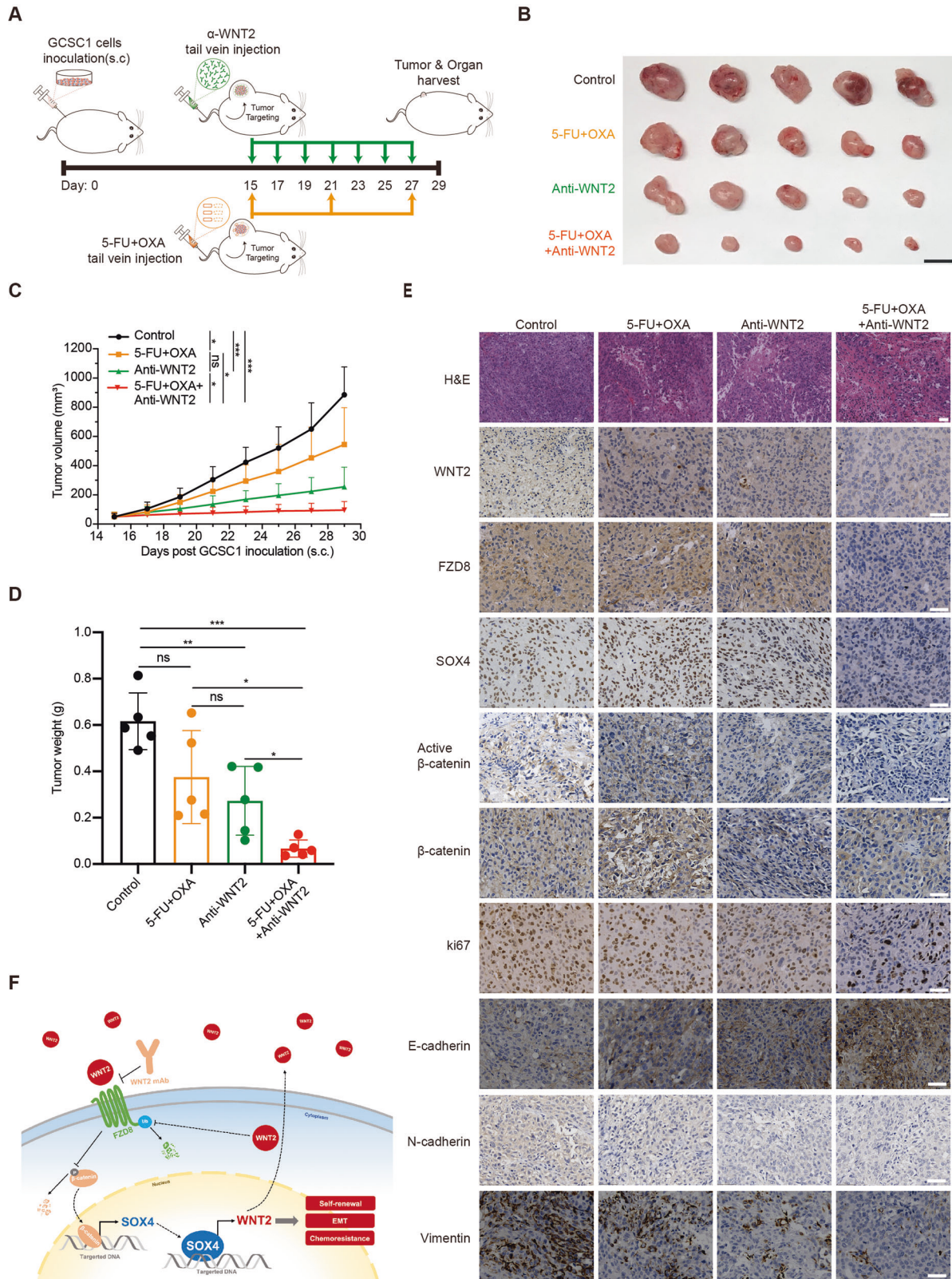


Fig. 6 Anti-WNT2 mAb treatment enhances the therapeutic efficacy of 5-FU plus OXA. **A** Schematic of anti-WNT2 or/and 5-FU plus OXA intervention in nude mice subcutaneously implanted with GCSCs ($n = 5$). **B** Photograph of GCSC xenograft tumors from indicated treatment groups; tumors were dissected from GCSC-injected mice at the end of the experiment; scale bar, 1 cm. **C** Tumor growth curves showing the development of GCSC xenografts in mice treated with saline + IgG (control), anti-WNT2 mAb or/and 5-FU + OXA. **D** Tumor weights of groups at the end of the experiment. **E** Tumor tissue from nude mice in the indicated treatment groups; H&E staining confirming malignant phenotype, and IHC staining of WNT2, FZD8, SOX4, active β -catenin, β -catenin, Ki67, E-cadherin, N-cadherin and Vimentin; scale bar, 50 μ m. **F** Schematic of WNT2-SOX4 auto-regulatory positive feedback loop maintenance of GCSC self-renewal and tumorigenic process. The error bars are presented as the means \pm SD. ns not significant; * $P < 0.05$; ** $P < 0.01$; *** $P < 0.001$; **** $P < 0.0001$.

three pathologists who are blinded to the clinical characteristics of each tissue point. The final immunoreactive score was determined by multiplying by the intensity and percentage score for each tissue point, as previously described [47]. Briefly, the staining intensity was scored as 0 (unstained), 1 (light yellow), 2 (brown yellow), and 3 (dark brown). The staining percentage scores as 0 (unstained), 1 (1%–25%), 2 (26%–50%), 3 (51%–75%), and 4 (76%–100%). If the total score was greater than or equal to the median score, it was considered a high WNT2 or SOX4 expression. The clinical characteristics of 95 GC patients and their correlations with WNT2 or SOX4 expression were summarized in Supplementary Tables S1 and S2.

For xenografts, all specimens freshly isolated from mice were immediately fixed in 4% paraformaldehyde. The paraffin-embedded samples were sectioned at 7 mm thickness. Followed by deparaffinization and rehydration, the sections were subjected to antigen retrieval by microwave heating for 20 min in 1 mM EDTA (pH 8.0) and blocked in 5% normal goat serum at 37 °C for 30 min. Subsequently, the tumor sections were incubated with primary antibodies specific to WNT2 (1:5, 000; Kexing Biotech, custom made), FZD8 (1:3, 000; Abcam, ab155093), SOX4 (1:5, 000; Abcam, ab86809), active β -catenin (1:2, 000; Cell Signaling Technology, cat.# 8814, Massachusetts, USA), β -catenin (1:300; Cell Signaling Technology, cat.# 8480), and Ki67 (1:2, 000; Cell Signaling Technology, cat.# 9449) overnight at 4 °C followed by incubation with a biotin-conjugated secondary antibody and streptavidin-HRP at 37 °C for 30 min. Finally, the sections were stained with DAB chromogen (Beyotime, P0202, Shanghai, China), and the cell nucleus was stained with hematoxylin for 5 min. The mouse tissue sections were subjected to similar deparaffinization, rehydration, and subsequent staining with H&E (Servicebio, Wuhan, China) for histological analysis. Images were captured with the Slide Scan System (SQS1000, TEKSQRAY, Shenzhen, China).

Double immunofluorescence (IF) staining

GCSC1 cells were dropped on chamber slides pre-treated with 0.075% (w/v) poly-L-lysine and fixed in 4% paraformaldehyde for 30 min at room temperature. The cells were permeabilized with 0.1% Triton X-100 in PBS for 15 min and blocked with 5% BSA in PBS for 30 min at room temperature. After washing with cold PBS, GCSC1 cells were followed by incubating with pre-mixed anti-WNT2 antibody (1:100; Kexing Biotech, custom-made,) and anti-SOX4 antibody (1:100; Abcam, ab86809) at 4 °C overnight. The pre-mixed goat anti-mouse IgG Fluor 488 secondary antibody (1:500; Abcam, ab150113) and donkey anti-rabbit IgG Fluor 647 secondary antibody (1:500; Abcam, ab150075) was performed in room temperature for 1 h, followed by nuclei staining of 4,6-diamidino-2-phenylindole (DAPI) with Prolong Gold Antifade Reagent (Cell Signaling Technology, 8961) for 10 min. For human GC samples, the tumor tissues were deparaffinated and rehydrated and the sections were subjected to antigen retrieval by microwave heating for 20 min in 1 mM EDTA (pH 8.0) and blocked in 5% normal goat serum at 37 °C for 30 min. Subsequently, the tumor sections were incubated with primary antibodies specific to WNT2 (1:100; Kexing Biotech, custom-made) and SOX4 (1:100; Abcam, ab86809) overnight at 4 °C followed by incubation with FITC/APC-conjugated secondary antibody at room temperature for 1 h. Finally, the sections were stained by DAPI with Prolong Gold Antifade Reagent (Cell Signaling Technology, 8961) for 10 min. The immunofluorescence images were visualized using the Confocal Laser Microscope System (Zeiss, LSM880).

Chromatin immunoprecipitation-qPCR assays

Chromatin immunoprecipitation (ChIP) experiments were conducted according to the manufacturer's instructions using an EZ ChIP kit (Merck Millipore, 17-371, Massachusetts, USA). Briefly, cells were cross-linked and pelleted, and the lysis supernatants were sonicated. The sonicated supernatants were incubated with Protein G beads, 10 μ g of antibodies against SOX4, or 10 μ g rabbit IgG antibody. The pulled-down and purified DNA fragments were detected by qPCR analysis with the primers listed in the Supplementary Materials. Relative enrichment was calculated as the amount of amplified DNA normalized to input.

Luciferase reporter assay

The luciferase reporter system was purchased from Promega Corporation (Dual-Glo Luciferase Assay System, Madison, Wisconsin, USA), and the assay was performed according to the manufacturer's instructions. Briefly, 100 ng of wild-type or mutated WNT2 reporter plasmid, 100 ng

SOX4 plasmid, 100 ng pGL3-Basic, and/or 10 ng pRL-SV40 plasmids were transfected into 293T cells with Lipofectamine 3000 (Invitrogen, California, USA). The activities of luciferase and Renilla were determined using confocal imaging and analysis (BioTek, Citation 3 system, Vermont, USA).

Animal studies

All animal procedures were approved by and conducted in accordance with the Animal Ethical and Welfare Committee of Shenzhen University and followed ARRIVE guidelines. BALB/c nude mice (aged 4–6 weeks; 20.0 ± 2.0 g; male) were purchased from Charles River Laboratories and maintained under specific pathogen-free conditions. sh-WNT2- or sh-NTC-transfected GCSC1/GCSC2 cells (2×10^5 cells in 0.2 mL PBS per mouse) were injected subcutaneously into the lower backs of the mice. The diameters of tumors and body weights were measured every other day. Tumor volume (mm^3) was measured using a Vernier caliper and calculated using the formula: volume = length \times width² \times 0.5. GCSC1 cells (2×10^5 cells per mouse) were injected subcutaneously into the lower backs of mice. Mice were randomly assigned into treatment groups (5 mice per group) when tumor diameters reached 5 mm (designated as day 1). Anti-WNT2 mAb [10 mg/kg/mouse; Kexing Biotech [25]] and/or 5-fluorouracil (5-FU) (10 mg/kg/mouse; MCE, California, USA) and oxaliplatin (OXA) (5 mg/kg/mouse; Selleck, Houston, TX, USA) were injected via the tail vein twice (5-FU + OXA) or three (anti-WNT2 mAb) times for one week. The corresponding control group was injected with the same volume of saline and/or IgG (10 mg/kg/mouse; Bio X cell, New Hampshire, USA). After mice were euthanized on day 29, tumors and organs (heart, lung, liver, spleen, kidney) were dissected from the indicated mice. As described below, paraffin-embedded sections were deparaffinized, and sections were examined by H&E and IHC staining.

Additional experimental procedures are provided in the Supplementary Information.

DATA AVAILABILITY

The GC scRNA-seq data used for the analysis of potential TFs regulating WNT2 gene expression in CD44+ CD54+ cells are available on the GEO database (accession number: GSE183904). R software is a free software environment for statistical computing and graphics (<https://www.r-project.org>). The data that support the findings of this study are available from the corresponding author upon reasonable request.

REFERENCES

- Sung H, Ferlay J, Siegel RL, Laversanne M, Soerjomataram I, Jemal A, et al. Global Cancer Statistics 2020: GLOBOCAN estimates of incidence and mortality worldwide for 36 cancers in 185 countries. *CA Cancer J Clin.* 2021;71:209–49.
- Smyth EC. Chemotherapy for resectable microsatellite instability-high gastric cancer? *Lancet Oncol.* 2020;21:204.
- Ajani JA. Evolving chemotherapy for advanced gastric cancer. *Oncologist.* 2005;10:49–58.
- Takaishi S, Okumura T, Wang TC. Gastric cancer stem cells. *J Clin Oncol.* 2008;26:2876–82.
- Prager BC, Xie Q, Bao S, Rich JN. Cancer stem cells: the architects of the tumor ecosystem. *Cell Stem Cell.* 2019;24:41–53.
- Ajani JA, Lee J, Sano T, Janjigian YY, Fan D, Song S. Gastric adenocarcinoma. *Nat Rev Dis Prim.* 2017;3:17036.
- Brungs D, Aghmesheh M, Vine KL, Becker TM, Carolan MG, Ranson M. Gastric cancer stem cells: evidence, potential markers, and clinical implications. *J Gastroenterol.* 2016;51:313–26.
- Smith LM, Nesterova A, Ryan MC, Duniho S, Jonas M, Anderson M, et al. CD133/prominin-1 is a potential therapeutic target for antibody-drug conjugates in hepatocellular and gastric cancers. *Br J Cancer.* 2008;99:100–9.
- Yoon C, Park DJ, Schmidt B, Thomas NJ, Lee H-J, Kim TS, et al. CD44 expression denotes a subpopulation of gastric cancer cells in which Hedgehog signaling promotes chemotherapy resistance. *Clin Cancer Res.* 2014;20:3974–88.
- Vugts DJ, Heuveling DA, Stigter-van Walsum M, Weigand S, Bergstrom M, van Dongen GAMS, et al. Preclinical evaluation of 89Zr-labeled anti-CD44 monoclonal antibody RG7356 in mice and cynomolgus monkeys: Prelude to Phase 1 clinical studies. *MAbs.* 2014;6:567–75.
- Malanchi I, Peinado H, Kassen D, Hussenet T, Metzger D, Chambon P, et al. Cutaneous cancer stem cell maintenance is dependent on beta-catenin signaling. *Nature.* 2008;452:650–3.
- Saygin C, Matei D, Majeti R, Reizes O, Lathia JD. Targeting cancer stemness in the clinic: from hype to hope. *Cell Stem Cell.* 2019;24:25–40.

13. Barker N, van Es JH, Kuipers J, Kujala P, van den Born M, Cozijnsen M, et al. Identification of stem cells in small intestine and colon by marker gene *Lgr5*. *Nature*. 2007;449:1003–7.
14. Munz M, Baeuerle PA, Gires O. The emerging role of EpCAM in cancer and stem cell signaling. *Cancer Res*. 2009;69:5627–9.
15. Yang L, Shi P, Zhao G, Xu J, Peng W, Zhang J, et al. Targeting cancer stem cell pathways for cancer therapy. *Signal Transduct Target Ther*. 2020;5:8.
16. Vider BZ, Zimmer A, Chastre E, Prevot S, Gespach C, Estlein D, et al. Evidence for the involvement of the *Wnt 2* gene in human colorectal cancer. *Oncogene*. 1996;12:153–8.
17. Mazieres J, You L, He B, Xu Z, Twogood S, Lee AY, et al. *Wnt2* as a new therapeutic target in malignant pleural mesothelioma. *Int J Cancer*. 2005;117:326–32.
18. Wang S, Zhang X, Li Z, Wang W, Li B, Huang X, et al. Circular RNA profile identifies *circOSBPL10* as an oncogenic factor and prognostic marker in gastric cancer. *Oncogene*. 2019;38:6985–7001.
19. Cao J, Zhang X, Xu P, Wang H, Wang S, Zhang L, et al. Circular RNA *circLMO7* acts as a microRNA-30a-3p sponge to promote gastric cancer progression via the *WNT2/β-catenin* pathway. *J Exp Clin Cancer Res*. 2021;40:6.
20. Cheng X-X, Wang Z-C, Chen X-Y, Sun Y, Kong Q-Y, Liu J, et al. Correlation of *Wnt-2* expression and beta-catenin intracellular accumulation in Chinese gastric cancers: relevance with tumour dissemination. *Cancer Lett*. 2005;223:339–47.
21. Goss AM, Tian Y, Tsukiyama T, Cohen ED, Zhou D, Lu MM, et al. *Wnt2/2b* and beta-catenin signaling are necessary and sufficient to specify lung progenitors in the foregut. *Dev Cell*. 2009;17:290–8.
22. Wang JCY. Evaluating therapeutic efficacy against cancer stem cells: new challenges posed by a new paradigm. *Cell Stem Cell*. 2007;1:497–501.
23. Battle E, Clevers H. Cancer stem cells revisited. *Nat Med*. 2017;23:1124–34.
24. Kahn M. *Wnt* signaling in stem cells and tumor stem cells. *Semin Reprod Med*. 2015;33:317–25.
25. Huang T-X, Tan X-Y, Huang H-S, Li Y-T, Liu B-L, Liu K-S, et al. Targeting cancer-associated fibroblast-secreted *WNT2* restores dendritic cell-mediated antitumour immunity. *Gut*. 2022;71:333–44.
26. Jin L, Luo C, Wu X, Li M, Wu S, Feng Y. *LncRNA-HAGLR* motivates triple negative breast cancer progression by regulation of *WNT2* via sponging *miR-335-3p*. *Aging*. 2021;13:19306–16.
27. Arteaga CL. Progress in breast cancer: overview. *Clin Cancer Res*. 2013;19:6353–9.
28. Kramer N, Schmöllerl J, Unger C, Nivarthi H, Rudisch A, Unterleuthner D, et al. Autocrine *WNT2* signaling in fibroblasts promotes colorectal cancer progression. *Oncogene*. 2017;36:5460–72.
29. Grunberg N, Pevsner-Fischer M, Goshen-Lago T, Diment J, Stein Y, Lavon H, et al. Cancer-associated fibroblasts promote aggressive gastric cancer phenotypes via heat shock factor 1-mediated secretion of extracellular vesicles. *Cancer Res*. 2021;81:1639–53.
30. Lin L, Wei H, Yi J, Xie B, Chen J, Zhou C, et al. Chronic *CagA*-positive *Helicobacter pylori* infection with *MNNG* stimulation synergistically induces mesenchymal and cancer stem cell-like properties in gastric mucosal epithelial cells. *J Cell Biochem*. 2019;120:17635–49.
31. Moreno CS. *SOX4*: the unappreciated oncogene. *Semin Cancer Biol*. 2020;67:57–64.
32. Scharer CD, McCabe CD, Ali-Seyed M, Berger MF, Bulyk ML, Moreno CS. Genome-wide promoter analysis of the *SOX4* transcriptional network in prostate cancer cells. *Cancer Res*. 2009;69:709–17.
33. Sinner D, Kordich JJ, Spence JR, Opoka R, Rankin S, Lin S-CJ, et al. *Sox17* and *Sox4* differentially regulate beta-catenin/T-cell factor activity and proliferation of colon carcinoma cells. *Mol Cell Biol*. 2007;27:7802–15.
34. Peng X, Liu G, Peng H, Chen A, Zha L, Wang Z. *SOX4* contributes to TGF-β-induced epithelial-mesenchymal transition and stem cell characteristics of gastric cancer cells. *Genes Dis*. 2018;5:49–61.
35. Zhan T, Rindtorff N, Boutros M. *Wnt* signaling in cancer. *Oncogene*. 2017;36:1461–73.
36. Vermeulen L, De Sousa E, Melo F, van der Heijden M, Cameron K, de Jong JH, et al. *Wnt* activity defines colon cancer stem cells and is regulated by the microenvironment. *Nat Cell Biol*. 2010;12:468–76.
37. Li Q, Ye L, Zhang X, Wang M, Lin C, Huang S, et al. *FZD8*, a target of *p53*, promotes bone metastasis in prostate cancer by activating canonical *Wnt/β-catenin* signaling. *Cancer Lett*. 2017;402:166–76.
38. Ajani JA, D'Amico TA, Bentrem DJ, Chao J, Cooke D, Corvera C, et al. Gastric cancer, version 2.2022, NCCN clinical practice guidelines in oncology. *J Natl Compr Canc Netw*. 2022;20:167–92.
39. Wang F, Zhang X, Li Y, Tang L, Qu X, Ying J, et al. The Chinese Society of Clinical Oncology (CSCO): clinical guidelines for the diagnosis and treatment of gastric cancer, 2021. *Cancer Commun*. 2021;41:747–95.
40. Janjigian YY, Shitara K, Moehler M, Garrido M, Salman P, Shen L, et al. First-line nivolumab plus chemotherapy versus chemotherapy alone for advanced gastric, gastro-oesophageal junction, and oesophageal adenocarcinoma (CheckMate 649): a randomised, open-label, phase 3 trial. *Lancet*. 2021;398:27–40.
41. Zhang S, Zhang H, Ghia EM, Huang J, Wu L, Zhang J, et al. Inhibition of chemotherapy resistant breast cancer stem cells by a *ROR1* specific antibody. *Proc Natl Acad Sci*. 2019;116:1370–7.
42. Kahn M. Can we safely target the *WNT* pathway? *Nat Rev Drug Discov*. 2014;13:513–32.
43. Visvader JE, Lindeman GJ. Cancer stem cells: current status and evolving complexities. *Cell Stem Cell*. 2012;10:717–28.
44. Clara JA, Monge C, Yang Y, Takebe N. Targeting signalling pathways and the immune microenvironment of cancer stem cells — a clinical update. *Nat Rev Clin Oncol*. 2020;17:204–32.
45. Chen J, Ju HL, Yuan XY, Wang TJ, Lai BQ. *SOX4* is a potential prognostic factor in human cancers: a systematic review and meta-analysis. *Clin Transl Oncol*. 2016;18:65–72.
46. Chen T, Yang K, Yu J, Meng W, Yuan D, Bi F, et al. Identification and expansion of cancer stem cells in tumor tissues and peripheral blood derived from gastric adenocarcinoma patients. *Cell Res*. 2012;22:248–58.
47. Detre S, Saclani Jotti G, Dowsett MA. “quickscore” method for immunohistochemical semiquantitation: validation for oestrogen receptor in breast carcinoma. *J Clin Pathol*. 1995;48:876–8.

ACKNOWLEDGEMENTS

We acknowledge Prof. Xianming Mo at Sichuan University for providing the GCSC cells. We thank Dr. Yunxiao Yang in Shenzhen University General Hospital for her assistance with the histological examination. This work was supported by grants from the National Natural Science Foundation of China (82173003 and 82073197), the Science and Technology Program of Guangdong Province in China (2019B030301009), the Industry and Information Technology Foundation of Shenzhen (20180309100135860), the Science and Technology Foundation of Shenzhen (JCYJ20200109113810154) and the Shenzhen Key Laboratory Foundation (ZDSYS20200811143757022).

AUTHOR CONTRIBUTIONS

Conceptualization, XYT and LF; methodology, XYT, YTL, and LF; investigation, XYT, YTL, HHL, LXM, CMZ, and LF; writing – original draft, XYT, and YTL; writing – review & editing, XYT, YTL, and LF; resources, XYT, YTL, HHL, LXM, CMZ, TTX, TXH and XDZ; formal analysis, XYT, YTL, and HHL; data curation, XYT, YTL, and HHL; visualization, XYT, YTL, HHL, CMZ; supervision, LF; funding acquisition, LF.

COMPETING INTERESTS

The authors declare no competing interests.

ADDITIONAL INFORMATION

Supplementary information The online version contains supplementary material available at <https://doi.org/10.1038/s41388-023-02816-1>.

Correspondence and requests for materials should be addressed to Li Fu.

Reprints and permission information is available at <http://www.nature.com/reprints>

Publisher's note Springer Nature remains neutral with regard to jurisdictional claims in published maps and institutional affiliations.

Springer Nature or its licensor (e.g. a society or other partner) holds exclusive rights to this article under a publishing agreement with the author(s) or other rightsholder(s); author self-archiving of the accepted manuscript version of this article is solely governed by the terms of such publishing agreement and applicable law.